Talanta 217 (2020) 121093

Contents lists available at ScienceDirect

Talanta

journal homepage: www.elsevier.com/locate/talanta

# Dual-modal label-free genosensor based on hemoglobin@gold nanocluster stabilized graphene nanosheets for the electrochemical detection of BCR/ABL fusion gene

Mojtaba Shamsipur[a,**], Leila Samandari[a], Leila Farzin[b,*], Fatemeh Molaabasi[c,d], Mohammad Hasan Mousazadeh[e]

[a] Department of Chemistry, Razi University, Kermanshah, Iran
[b] Department of Analytical Chemistry, School of Chemistry, College of Science, University of Tehran, Tehran, Iran
[c] Department of Chemistry, Tarbiat Modares University, Tehran, Iran
[d] Department of Biomaterials and Tissue Engineering, Breast Cancer Research Center, Motamed Cancer Institute, ACECR, Tehran, Iran
[e] Department of Chemistry, Amirkabir University of Technology, Tehran, Iran

ARTICLE INFO

*Keywords:*
Chronic myelogenous leukemia
DNA-based biosensor
Graphene
Liquid phase exfoliation
Signal off/on modes

ABSTRACT

For the first time, we have successfully synthesized stable graphene nanosheets from graphite powder through sonication in the **hemoglobin-capped gold nanoclusters** (Hb@AuNCs) solution for biosensing application. This approach, as a simple method for the exfoliation and fragmentation of graphite in a nanocluster solution, enabled us to produce stable aqueous graphene dispersions at low cost and without the need for hazardous chemicals or tedious experimental procedures. In this method, Hb@AuNCs were used not only as stabilizing agent of graphene through non-covalent bonding, but also as dispersing agent of few-layer graphene nanosheets. The Hb@AuNCs stabilized graphene (Hb@AuNCs-G) was characterized by high resolution transmission electron microscopy (HRTEM), zeta-sizer and Raman spectroscopy. Then, the graphene nanosheets were applied as a novel versatile electrochemical platform for ultrasensitive biosensing of short DNA species of chronic myelogenous leukemia (CML) based on the "signal off" and "signal on" strategies. For this purpose, a single strand DNA (ssDNA) was immobilized on the Hb@AuNCs-G/AuNPs modified electrode surface and acted as the bior-ecognition element. Methylene blue (MB), as the signaling probe, was then intercalated into the ssDNA. The intercalated MB was liberated upon interaction with the synthetic complementary DNA (cDNA, target), thereby resulting in the apparent reduction of MB redox signal. This designed "signal off" sensing system enabled the voltammetric determination of the target cDNA over a dynamic linear range (DLR) of 0.1 fM to 10 pM with a limit of detection (LOD) of 0.037 fM. In the "signal on" strategy, the response to the cDNA was detected by monitoring the change in the electron transfer resistance ($R_{ct}$) using the ferro/ferricyanide system as a redox probe. The charge transfer resistance of the probe was found to increase linearly with increasing concentration of target cDNA in the range of 0.1 fM–10 pM with a limit of detection of 0.030 fM. Finally, the selectivity and feasibility of genosensor was evaluated by the analysis of derived nucleotides from mismatched sequences and the clinical samples of patients with leukemia as real samples, respectively.

## 1. Introduction

Among various problems faced by mankind, health-related concerns are prevailing since long, as they are commonly found in the form of chromosomal disorders. The chronic myelogenous leukemia (CML) is a slow-progressing leukemia associated with a specific genetic abnormality in the leukemia cell, called as the Philadelphia chromosome (Ph). The cytogenetic hallmark of CML is the Ph chromosome resulting from a balanced translocation between chromosomes 9 and 22 which leads to the formation of the BCR/ABL fusion gene. The presence of this translocation is a highly sensitive test for CML, since all cases of CML are positive for BCR-ABL. The methods reported for gene fusion identification are mainly molecular techniques. The fluorescent in situ hybridization (FISH) is a technique that allows the narrowing of

* Corresponding author.
** Corresponding author.
*E-mail addresses:* mshamsipur@yahoo.com (M. Shamsipur), lfarzin84@yahoo.com (L. Farzin).

https://doi.org/10.1016/j.talanta.2020.121093
Received 28 February 2020; Received in revised form 23 April 2020; Accepted 25 April 2020
Available online 29 April 2020
0039-9140/ 

breakpoint regions for hundreds of Kilobases [1]. Additionally, the real-time polymerase chain reaction (PCR) [2] and flow cytometry immunophenotyping [3] can be used as new alternatives, offering good sensibility and specificity as compared to chromosomal banding. However, these are high-cost techniques and require specialized technicians. In addition, these techniques exhibit obstacles such as difficulty in obtaining metaphase chromosome spreads for specific types of tumors and growth problems of some lineage cells in vitro.

In recent years, a new evolving technology called "genosensor" has shown an enormous potential and has constantly complimented the conventional diagnoses. The genosensor technology offers a wide potential of applicability to clinical and laboratory diagnosis, allowing a direct real-time analysis of nucleic acid targets with low-cost, compared to other available methods [4]. Up to now, a wide range of genosensors equipped with various transducers (such as electrochemical, optical, photoacoustic, magnetoelastic, etc) has been developed for BCR/ABL fusion gene detection [4]. Among these methods, the electrochemical genosensors have been introduced for developing easy-to-use and miniaturized devices for the ultrasensitive monitoring of chromosomal abnormalities [5-11]. It is worth mentioning that the nanotechnology has played an important role for innovation and development of such new electrochemical biosensing strategies.

Graphene and its derivatives have been hailed by many scientists as the "wonder material" of the 21st century, especially for biological applications. The potential of using graphene to design electrochemical biosensing devices is amazing because of all of the interesting traits of this carbon-based nanomaterial. One of the main features of graphene which attracted the attention of electrochemists is its impressive electrical conductivity. Graphene is incredibly conductive, as far as it can be used for sensitive recording of electrical signals of the neurons in the medical field [12]. In addition, the high surface to volume of graphene makes it a suitable modifier for the electrode surface. However, pristine graphene nanosheets are unstable in aqueous media and tend to aggregate because of the van der Waals interactions [13]. A commonly used approach to make stable graphene for the electrochemical applications is chemical oxidation of commercial graphite powder into graphite oxide, followed by the exfoliation of graphite oxide in distilled water using the ultrasound frequency and then reduction of graphene oxide (GO) to its reduced form [14]. However, the production and reduction of GO require the use of toxic or explosive chemicals, such as sulfuric acid, hydrazine, and potassium permanganate, or long and complicated processes. In addition, the crystalline structure and electronic properties of the synthesized graphene are not well preserved because of the formation of defects and the remaining chemical groups in graphene [15]. In fact, the doughty chemical oxidation destroys the electronic structure of graphene and limits its application in the microelectronics, etc. Therefore, the preparation of stable, electro-conductive and processable aqueous graphene dispersions using a facile and green approach for the electrochemical biosensing assays has thus far remained as a challenge. The liquid-phase exfoliation (LPE) of graphite powder in the presence of exogenous materials (e.g., organic solvent, ionic liquids, surfactants) using a sonication procedure, and sometimes by additional experimental steps such as the use of electrochemical potentials, is a promising cost-effective method for scalable production of conductive single- or few-layer graphene through simple and available devices [16,17].

Since 2008, when the LPE of graphite through the sonication of graphite powder in *N*-methylpyrrolidone was first proposed by Coleman et al. [18], a huge progress has been made in the past decade. Despite high quality of as-produced graphene, the toxicity and lack of biocompatibility of the used materials have restricted its safe use in biomedical applications. Therefore, the exploration of new green cost-efficient exfoliation media is urgent and vital. In this regard, Khademhasseini and co-workers [13] proposed a facile, green and inexpensive approach for preparing stable aqueous graphene dispersions, which involves the exfoliation and fragmentation of graphite into graphene through sonication in bovine serum albumin (BSA) aqueous solution. Graphite is a ubiquitous and natural material, and BSA is a natural protein derived from cow. The use of this approach results in the production of unfunctionalized and non-oxidized graphene sheets.

Similar to the above mentioned study, for the first time, in this work we synthesized graphene nanosheets by sonication of graphite powder in **hemoglobin-capped gold nanoclusters** (Hb@AuNCs); to obtain Hb@AuNCs stabilized graphene (Hb@AuNCs-G) adduct as a nanoplatform with high affinity for biomolecules. Electrochemical sensing interfaces based on protein-stabilized metal NCs have attracted great interest because they provide simple green reaction processing, biocompatibility, core/shell architecture, and good conductivity [19-21]. Using a protein as the protecting/reducing agent has the advantage that can be functionalized smoothly and efficiently through its amine and carboxyl groups.

In the present study, a project has been undertaken for developing an electrochemical dual-mode sensing method based on the Hb@AuNCs-G for BCR/ABL fusion gene detection. The stable aqueous graphene dispersions synthesized through LPE of graphite powder in the presence of Hb@AuNCs have a good capacity for immobilization of ssDNA receptors due to the high surface to volume ratio of graphene and functional groups of hemoglobin. For the further enhancement of the electrode surface and its electro-conductivity, Hb@AuNCs-G was assembeled on the gold nanoparticles (AuNPs) modified electrode. Interestingly, the high conductivity of AuNPs increased the electron transfer between the active centers of bioreceptors and electrodes and, thus, they acted as electron transfer "electron wires" [22]. In 1996, for the first time, Brown et al. proved the direct electron transfer between the electrode and the protein by AuNPs [23]. They found that the nanometer-scale morphology of metals was closely related to the protein electrochemistry.

## 2. Experimental

### 2.1. Reagents and chemicals

Hemoglobin (Hb) was extracted and purified from the fresh blood of one of the authors. Sodium tetrachloroaurate(III) dihydrate ($NaAuCl_4.2H_2O$, 99.0%), potassium hexacyanoferrate(III) ($K_3Fe(CN)_6$, ≥99.0%), potassium hexacyanoferrate(II) trihydrate ($K_4Fe(CN)_6.3H_2O$, ≥99.95%), *N*-hydroxysuccinimide (NHS), 1-ethyl-3-(3-dimethylaminopropyl) carbodiimide hydrochloride (EDC), potassium chloride (≥99%), sodium chloride (≥99%), methylene blue trihydrate (MB, 85%) and Tris-HCl buffer were purchased from Sigma-Aldrich (USA). Natural graphite powder was supplied by Merck (Germany). The 18 mer-oligonucleotides used in this work were synthesized by Faza Biotech Company (Iran) according to specific sequences of BCR/ABL gene as follows:

Probe ssDNA (pDNA): 5′-$NH_2(CH_2)_6$ AGA GTT CAA AAG CCC TTC-3′

Target DNA or complementary DNA (cDNA): 5′-GAA GGG CTT TTG AAC TCT-3′

Singele-base mismatched DNA (sbmDNA): 5′-GAA GGG CAT TTG AAC TCT-3′

Non-complementary DNA (ncDNA): 5′-CTT CCC GAA AAC TTC AGA-3′.

The EIS experiments were carried out in Tris–HCl buffer (pH 7.0) containing 5 mM $K_3[Fe(CN)_6]/K_4[Fe(CN)_6]$ (1:1)/0.1M KCl with a frequency range of 0.1 Hz-50 kHz and an Ac voltage of 10 mV.

The DPV measurements were carried out in Tris–HCl buffer (pH 7.0) containing 50 mM NaCl in a range of 0.1 to -0.6 V with the amplitude of 10 mV at a scan rate of 50 mV $s^{-1}$.

### 2.2. Apparatus

Differential pulse voltammetry (DPV), electrochemical impedance

spectroscopy (EIS) and cyclic voltammetry (CV) measurements were performed with a PalmSens instrument (PalmSens BV, Netherlands) which is controlled by computer. The working electrode was a modified glassy carbon electrode (i.d = 3.0 mm), and auxiliary and reference electrodes were a Pt wire and Ag/AgCl electrode (KCl, 3 M), respectively. The TEM and HRTEM characterizations were performed on a Tecnai G2 F20 (Philips, Netherlands) and a JEM-2200FS (JEOL, Japan) operating at 200 kV, respectively. Samples for recording TEM images were prepared by drop casting of solution on carbon coated copper grids and dried at room temperature. The hydrodynamic sizes and the surface charges of the nanoclusters in an aqueous solution were measured using a Zetasizer nano ZS series dynamic light scattering (DLS) (Malvern Instruments Ltd, UK). A 780 pH Meter was used for measuring pH at 25 °C (Metrohm, Switzerland). A sonoreactor UTR200 (Hielscher, Germany) with maximum output power of 200 W, operating frequency of 24 kHz and ultrasonic intensity of 80 W $cm^{-2}$ was employed for ultrasound-assisted exfoliation of graphite oxide.

### 2.3. Synthesis of hemoglobin-capped Au nanoclusters

The Hb@AuNCs were synthesized according to our previous procedure [24] through a one-step green reduction from $HAuCl_4$ (2.5 mL, 2.8 mM) and stabilized by Hb protein (2.5 mL, 7.0 mg $mL^{-1}$) at 37 °C under basic conditions (pH ~12.4) with vigorous stirring for 24 h, followed by centrifuging to remove any suspended or larger particle sizes in the Hb@AuNCs solution.

### 2.4. Preparation of stable aqueous graphene dispersion

In this work, graphite was exfoliated and broken down to graphene under sonication conditions in an aqueous Hb@AuNCs solution (Fig. 1). For this purpose, 0.1 g of graphite powder was dispersed in 10 mL of the aqueous Hb@AuNCs solution. The mixture was then sonicated for 7 h while being mixed with a magnetic stirrer. The acoustic cavitation of ultrasonic waves led to the formation, development and collapse of bubbles in the water, which induced shock waves on the graphite that resulted in its exfoliation and fragmentation. Subsequently, the few-layer graphene nanosheets interacted with the Hb molecules, which stabilized them in the water. In fact, the large surface area of hydrophobic graphene enabled the effective adsorption of the hydrophobic segments of Hb, while the hydrophilic segments of Hb interacted with the water.

The sonicated mixture was allowed to stand for ~ 24 h to allow some of the large graphene aggregates and graphite particles to settle prior to separation of the dark supernatant from the sediment. The mixture was centrifuged at 3000 rpm for 30 min. After an initial centrifugation, there was stable aqueous graphene dispersion without any aggregation or precipitation of graphene.

### 2.5. Preparation of "signal on" and "signal off" electrochemical genosensors

Glassy carbon electrode was polished with 0.05 μm alumina slurry on a polishing cloth and then ultrasonicated in water-ethanol solution (1:1) to remove adsorbed particles. The gold nanoparticles (AuNPs) were electrochemically deposited on GCE using chronoamperometry method through immersed electrode in 1 mM $NaAuCl_4$ solution containing 0.1 M KCl by applying a potential of -0.2 V for 30 s. The electrode was washed with double distilled water and dried in the air. Subsequently, 10 μL of Hb@AuNCs-G solution was dropped onto the surface of AuNPs/GCE and allowed to dry in a refrigerator. After washing the electrode surface, 20 μL of an aqueous solution containing 10 mM of EDC and 20 mM of NHS was dropped onto the modified electrode and and kept for 1 hour to activate the carboxylic groups on the nanoclusters. Finally, after washing the electrode surface, 5 μL of the pDNA (1 μM) was placed on the Hb@AuNCs-G/AuNPs/GC electrode surface and remained for 2 hours.

To design "signal on" strategy, the hybridization reaction between two DNA strands was performed by dropping of 5 μL of different

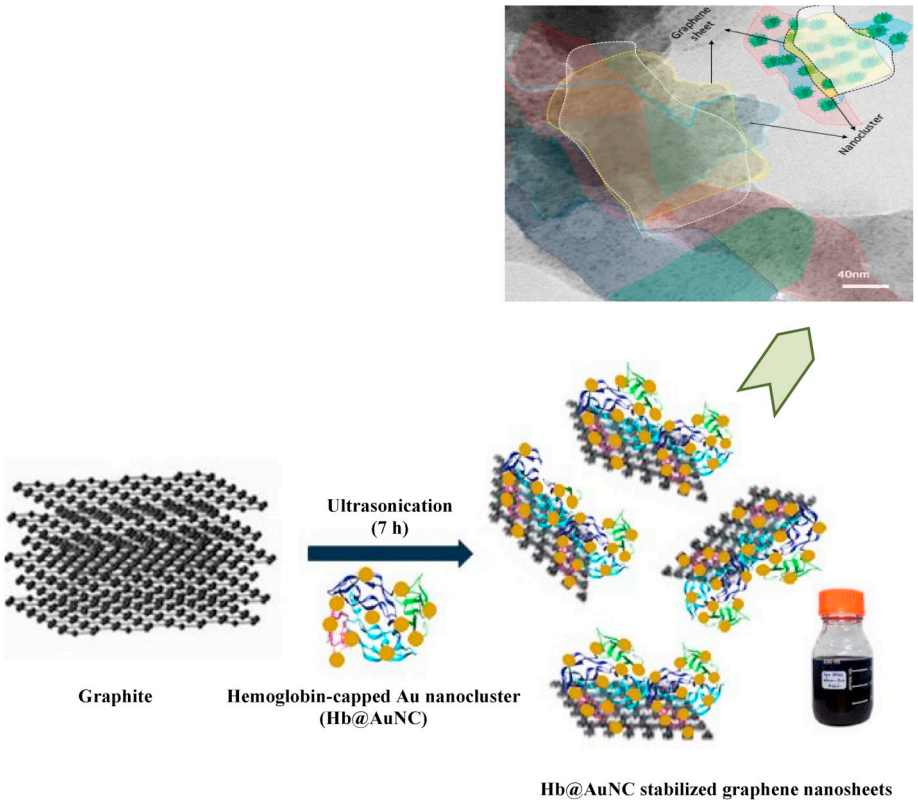


**Fig. 1.** Schematic illustration of synthesis procegure of Hb@AuNCs stabilized graphene.

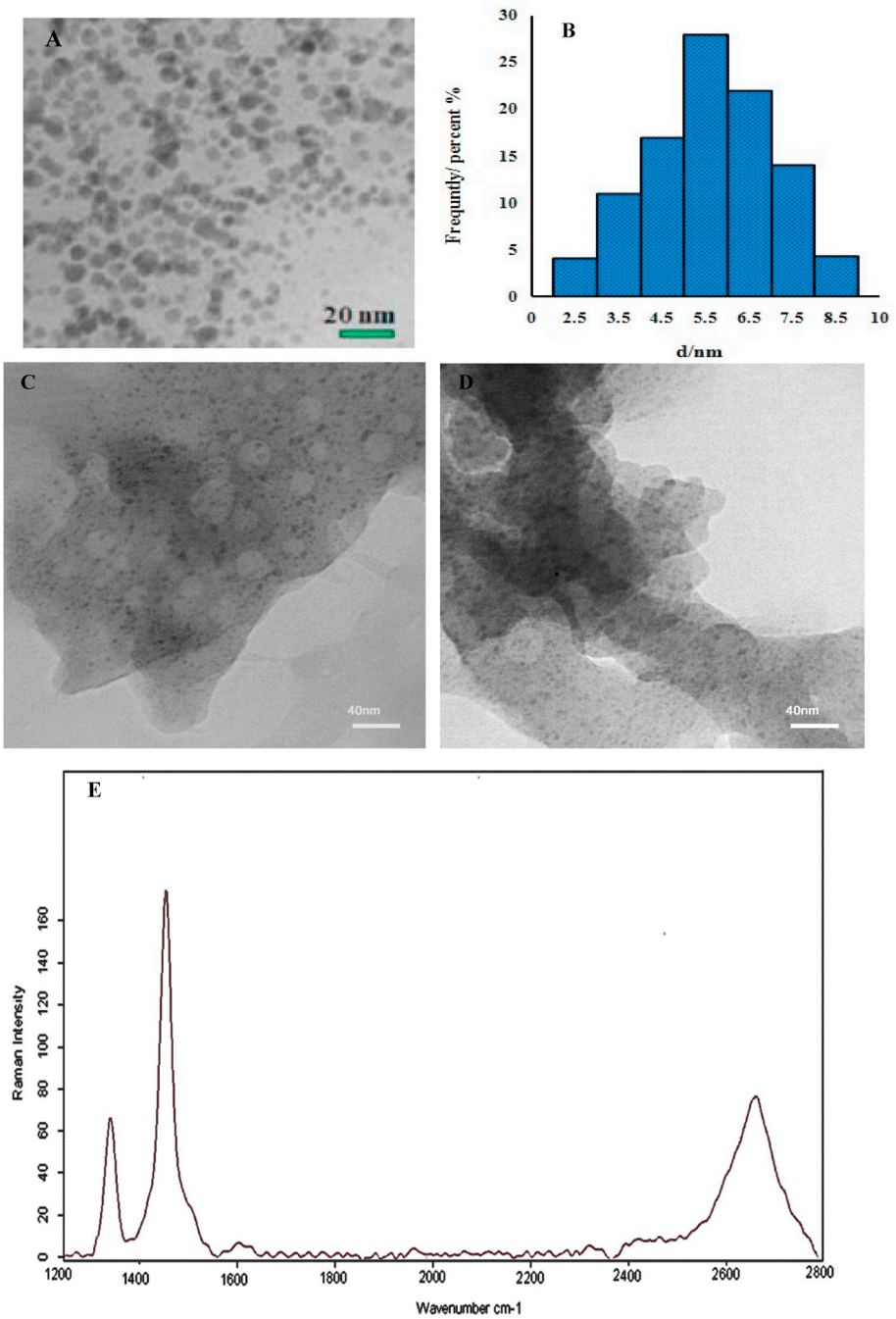


**Fig. 2.** (A) TEM image and (B) corresponding size histogram of as-prepared Hb@AuNCs based on a count of 130 particles; (C) and (D) TEM images of Hb@AuNCs stabilized graphene nanosheets; (E) Raman spectrum for graphene. The D, G, and 2D bands were detectable.

concentrations of target DNA onto the modified electrode surface and allowed to react for 30 min. Then, the label-free detection of DNA hybridization was performed with EIS measurements in Tris–HCl buffer (pH 7.0) containing 5 mM $K_3[Fe(CN)_6]/K_4[Fe(CN)_6]$ (1:1)/0.1M KCl.

Methylene blue was also used as the electrochemical indicator for monitoring the hybridization reaction following the hybridization of the target DNA sequence. Based on previous reports, MB can specifically bind with guanine bases in ssDNA [19], and the pDNA used here is an ssDNA type which is rich of guanine bases. For fabrication of MB-pDNA/HB@AuNCs-G/AuNPs/GCE for "signal off" determination of target DNA, the end of modified electrode was immersed in Tris–HCl buffer (pH 7.0) containing 20 μM MB and 50 mM NaCl for 10 min under stirring at room temperature. After rinsing with buffer, 5 μL of a fixed concentration of target cDNA was dropped onto the electrode surface to react for 30 min. In this step, the target nucleic acids were immobilized on the MB-pDNA/HB@AuNCs-G/AuNPs/GC electrode surface through DNA hybridization reaction. Upon the introduction of target cDNA, the MB molecules were liberated from the modified electrode surface along with the hybridization reaction. After washing with buffer to remove unbound target cDNA, DPV responses of the genosensor were recorded in Tris–HCl buffer (pH 7.0) solution. In fact, DPV was used for detection of electrochemical response of MB as a redox indicator of the hybridization event.

Overall, the change of electrochemical responses of MB bound to the pDNA and $[Fe(CN)_6]^{3-/4-}$ probe in the solution as a result of DNA hybridization process allows an "off"-"on" genosensor development.

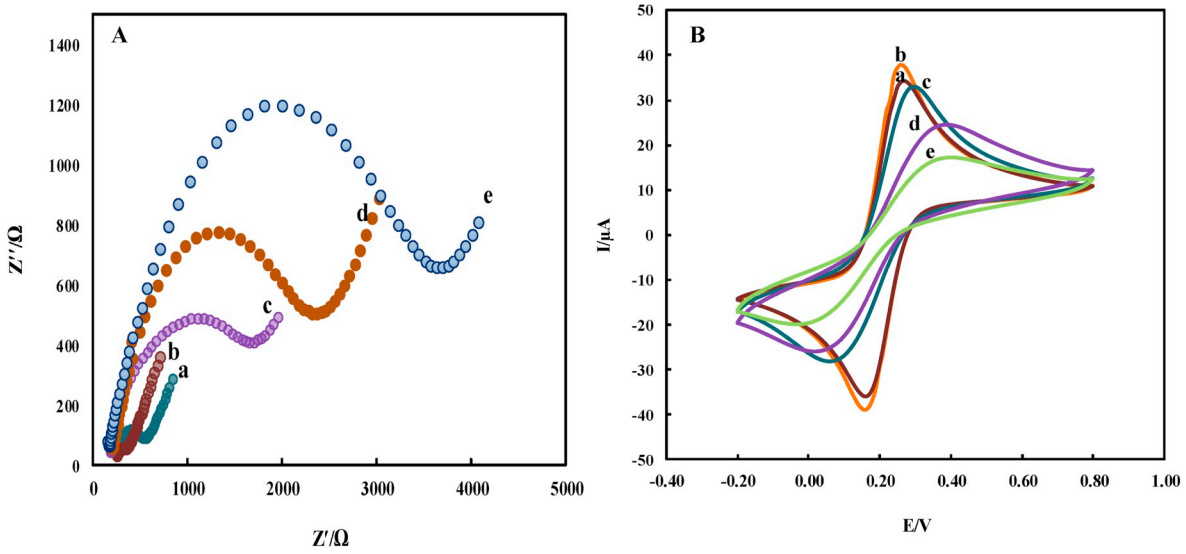


**Fig. 3.** Electrochemical characterization of genosensor by (A) Nyquist plots and (B) CVs of bare GCE (a), AuNPs (b), Hb@AuNCs/AuNPs/GCE (c), pDNA/Hb@AuNCs/AuNPs/GCE (d), cDNA/pDNA/Hb@AuNCs/AuNPs/GCE (e) in Tris–HCl buffer (pH 7.0) containing 5 mM $K_3[Fe(CN)_6]/K_4[Fe(CN)_6]$ (1:1)/0.1M KCl. The bias potential for EIS is 0.18 V.

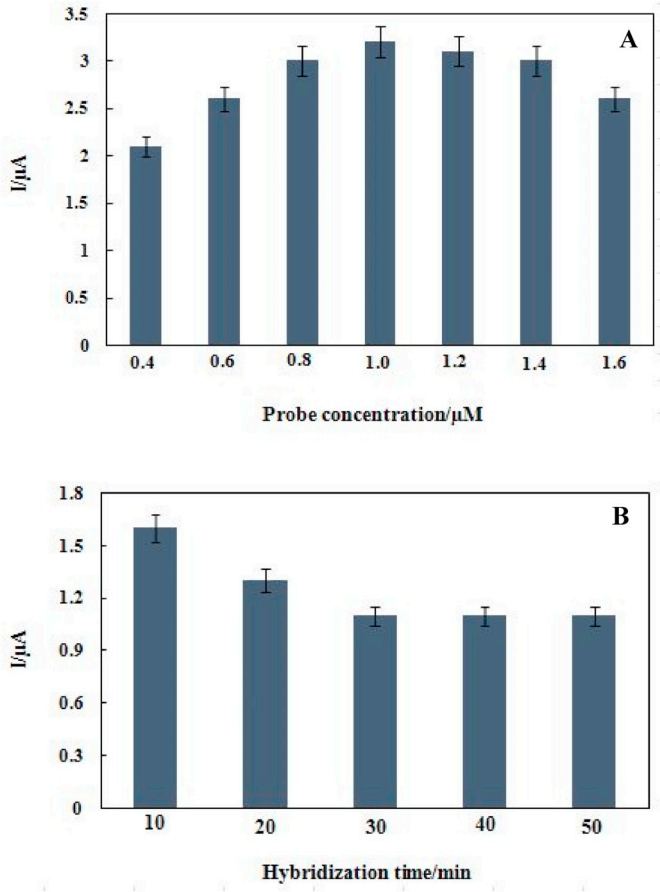


**Fig. 4.** Effect of (A) concentration of pDNA and (B) hybridization time of pDNA (1.0 μM) to cDNA (0.1 pM) on the DPV responses of MB in Tris–HCl buffer (pH 7.0) containing 50 mM.

## 3. Results and discussion

### 3.1. Characterization of nanomaterials

The representative TEM image of the Hb@AuNCs was displayed in Fig. 2A. As seen, the average size of Hb@AuNCs was approximately 5 nm. The particle size of nanoclusters was also supported by determination of hydrodynamic diameter ($D_H$). The DLS results revealed an average $D_H$ of 5.6 ± 0.5 nm (Fig. 2B). According to the results obtained using the Zetasizer technique, the average zeta potential of the nanoclusters shifted towards negative values by almost 32 mV. It is presumably a consequence of the presence of negatively charged carboxyl groups in the Hb-capped AuNCs at pH 7. After the graphite powder was mixed with the nanocluster solution and the mixture was sonicated for 7 h, a homogeneous and dense coverage of AuNCs was conformed on the GO surface. The TEM images of the Hb@AuNCs-G (Fig. 2C and D) showed the successful isolation of graphene nanosheets without any aggregation of GO sheets or free AuNCs. The Raman spectrum of the synthesized graphene (Fig. 2E) clearly showed the D, G, and 2D bands at ~1330 $cm^{-1}$, ~1500 $cm^{-1}$ and ~2700 $cm^{-1}$, respectively. These observations confirm the high quality of the synthesize graphene.

### 3.2. Electrochemical characterization of genosensor based on EIS and CV methods

The procedure of electrode modification is tailored to control the charge transfer rates for specific applications such as development of sensors/biosensors. Therefore, the electrochemical characterization of the modified electrodes toward developing a biosensor is of vital importance. The used methods are usually based upon the charge-transfer properties of the compounds immobilized on the electrode surface. Because that the most of chemical/biochemical compounds are electroinactive, the electron transfer redox probes are used to investigate the step-by-step modification of electrodes. For this purpose, the electrochemical responses of the bare/unmodified GCE and modified electrodes were benchmarked and characterized using the $[Fe(CN)_6]^{3-/4-}$ couple as a suitable electrochemical probe in solution.

At first, EIS method was carried out in Tris–HCl buffer (pH 7.0) containing 5 mM $K_3[Fe(CN)_6]/K_4[Fe(CN)_6]$ (1:1)/0.1 M KCl. Fig. 3A shows the Nyquist plots of impedance spectra at the GCE during the modification step. The bare GCE exhibited a very small semicircle at high frequency (curve a, $R_{ct}$ = 508 Ω), indicating good electron transfer of the system. When AuNPs were electro-deposited on the surface of GCE, the electrochemical semicircle became much smaller and close to a straight line (curve b, $R_{ct}$ = 152 Ω), which shows the

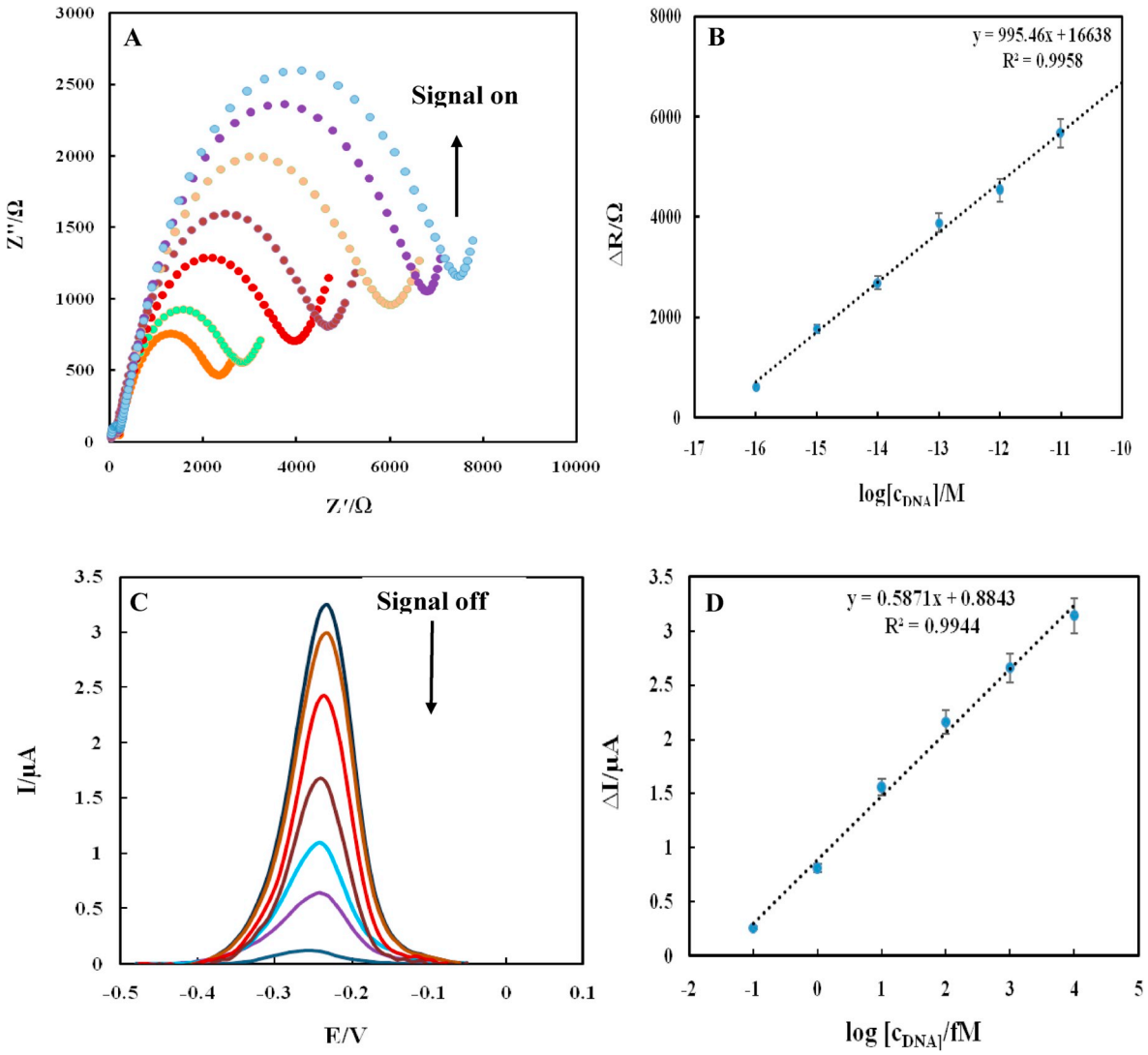


**Fig. 5.** (A) Nyquist plots of the pDNA/Hb@AuNCs/AuNPs/GCE incubated with different concentrations of target cDNA (0, 0.1 fM, 1 fM, 10 fM, 100 fM, 1 pM, 10 pM) in Tris–HCl buffer (pH 7.0) containing 5 mM $K_3[Fe(CN)_6]/K_4[Fe(CN)_6]$ (1:1)/0.1M KCl (1:1); (B) the calibration curves of $\Delta R_{ct}$ versus target cDNA concentration from 0.1 fM to 10 pM; (C) DPV responses of the MB-pDNA/Hb@AuNCs/AuNPs/GCE incubated with different concentrations of target cDNA (0, 0.1 fM, 1 fM, 10 fM, 100 fM, 1 pM, 10 pM) in Tris–HCl buffer (pH 7.0) containing 50 mM NaCl; (D) the calibration curves of DPV peak current versus the logarithm of cDNA concentration from 0.1 fM to 10 pM.

improved electron transfer of the electrode. This is due to the fact that most of metallic nanoparticles successfully improve electron transfer rate resulting in smaller charge transfer resistance. The assembling of Hb@AuNCs-G on the AuNPs formed a stable film on the electrode surface and provided a large specific surface area for immobilization of larger number of ssDNA through activation of the carboxyl groups with water-soluble EDC/NHS. However, the formation of this conductive nanolayer was resulted in a large enhancement in $R_{ct}$ (curve c, $R_{ct}$ = 1974 Ω) due to electrostatic attraction between $[Fe(CN)_6]^{3-/4-}$ anions and the negatively charged graphene. In fact, such significant increase in the charge transfer resistance of Hb@AuNC-G/AuNP/GCE with respect to the bare GCE confirmed the presence of negatively charged carboxyl groups on the nanocomposite surface. When, the pDNA strands were covalently self-assembled onto the nanoclusters, the $R_{ct}$ value was furthered increased significantly (curve d, $R_{ct}$ = 2397 Ω). It can be attributed to the fact that the negatively-charged DNA probes act as an electrostatic barrier to repel the $[Fe(CN)_6]^{3-/4-}$ probe and hinder its interfacial electron transfer reaction. Generally, the nucleic acids with negative charges on their phosphate backbone make an electrostatic repulsive force on $[Fe(CN)_6]^{3-/4-}$ probe. Finally, after the incubation of cDNA with pDNA, the $R_{ct}$ showed a further increase (curve e, $R_{ct}$ = 4175 Ω) which called a "signal on" response.

The electrochemical behavior of the modified electrode was further investigated by recording its cyclic voltammograms in Tris–HCl buffer (pH 7.0) solution containing 5 mM $K_3[Fe(CN)_6]/K_4[Fe(CN)_6]$ (1:1)/ 0.1 M KCl (Fig. 3B). As expected, the cyclic voltammogram displayed a reversible behavior at the bare GCE with a peak-to-peak separation of 70 mV (curve a). After the electrodeposition of AuNPs at the GCE surface, the electrode exhibited an increase in the peak current (curve b) compared to the bare electrode. It suggests that the electrodeposited AuNPs layer accelerates the electron transfer, which is consistent with the EIS results for this step. However, the assembling of Hb@AuNCs-G on the AuNPs/GCE decreased the peak current (curve c). Finally, the immobilization of pDNA on the modified electrode surface and last hybridization of cDNA resulted in a significant decrease in CV signals (curve d and curve e), implying a "signal off" strategy. All these results are consistent with the change in surface property of the GCE in the course of the successive modification steps.

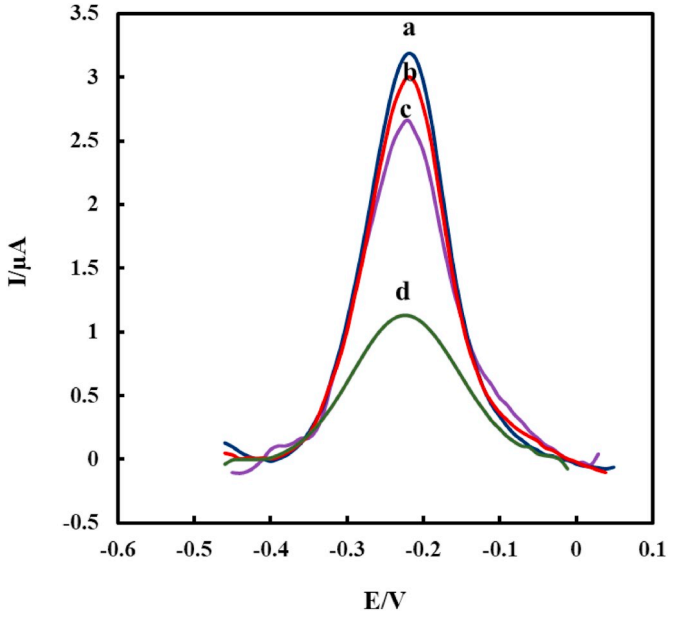


**Fig. 6.** DPV signals of MB-cDNA/pDNA/Hb@AuNCs/AuNPs/GCE for (a) no sequence, (b) ncDNA (1.0 pM), (c) sbmDNA (1.0 pM) and (D) cDNA (0.1 pM).

**Table 1**
The obtained results from cDNA analysis of real sample by the signal on genosensor.

| Sample | Added cDNA | [a]Found cDNA | RSD (%) | Recovery (%) |
|---|---|---|---|---|
| 1 | $5.00 \times 10^{-16}$ | $4.75 \times 10^{-16}$ | 3.9 | 95 |
| 2 | $1.00 \times 10^{-14}$ | $0.98 \times 10^{-14}$ | 5.8 | 98 |
| 3 | $25.00 \times 10^{-13}$ | $23.9 \times 10^{-13}$ | 3.8 | 96 |

[a] Calculated as a mean of four measurements.

**Table 2**
The obtained results from cDNA analysis of real sample by the signal off genosensor.

| Sample | Added cDNA | [a]Found cDNA | RSD (%) | Recovery (%) |
|---|---|---|---|---|
| 1 | $5.00 \times 10^{-16}$ | $5.10 \times 10^{-16}$ | 4.8 | 102 |
| 2 | $1.00 \times 10^{-14}$ | $0.97 \times 10^{-14}$ | 5.6 | 97 |
| 3 | $5.00 \times 10^{-13}$ | $4.95 \times 10^{-13}$ | 4.2 | 99 |

[a] Calculated as a mean of four measurements.

### 3.3. Optimization of effective parameters on the genosensor response

The electrochemical responses of a genosensor can be influenced by several experimental parameters that should be optimised in order to obtain better performances. Among the experimental parameters, the surface probe ssDNA density is a vital influencing factor on the response of genosensors [25]. Since the probe density can be controlled by varying concentration of the pDNA used in sensor fabrication, the influence of this parameter on the response of the prepared sensor was studied and the results were shown in Fig. 4A. As seen, the current of absorbed MB increased with increasing concentration of loaded pDNA on the surface of modified electrode up to 1 μM. However, the higher concentrations of probe ssDNA led to reduction of the MB signals, owing to the saturation of electrode surface and the consequent steric resistance.

Since the hybridization time is a vital influencing factor on the response of genosensors, the effect of this parameter on the sensor response was also investigated (Fig. 4B). As is obvious, the current response decreased rapidly with increasing hybridization time up to 30 min and then leveled off at higher time periods, suggesting that the formation of dsDNA at the electrode surface has reached to a saturation level.

### 3.4. Analytical performance of dual-modal label-free genosensor

The designed genosensor was employed for the determination of target DNA using EIS and DPV methods. Fig. 5A shows the Nyquist plots of impedance spectra on the surface of pDNA/Hb@AuNC-G/AuNPs/GCE in the presence of $[Fe(CN)_6]^{3-/4-}$ after being exposed to different concentrations of target cDNA (i.e., 0, 0.1 fM, 1 fM, 10 fM, 100 fM, 1 pM, 10 pM), which clearly indicates a "signal on" strategy. As is obvious, when the hybridization of two strands occurs, the electrostatic repulsion between $[Fe(CN)_6]^{3-/4-}$ and DNA strand will increase. Hence, the $R_{ct}$ value is increased with increasing number of pDNA-cDNA conjugates, due to creation of a barrier in electron transfer process of the $[Fe(CN)_6]^{3-/4-}$ probe at the surface of modified electrode. Based on such "signal on" trend (Fig. 5B), the genosensor exhibited a good linear response to target DNA in the concentration range of 0.1 fM–10 pM with a regression equation of $\Delta R\ (\Omega) = 995.46 \log_{(cDNA)} (M) + 16638$ ($R^2 = 0.9958$) (n = 6) and a LOD of 0.030 fM (based as 3σ, where σ is the standard deviation of the blank).

Based on the "signal off" strategy, the MB adsorbed by the probe ssDNA will be released from the electrode surface along with hybridization reaction and, therefore, the current signal of MB is decreased. As it mentioned, MB is easy to anchor on ssDNA modified electrode by the interaction between MB and guanine bases of ssDNA. Thus, a large redox peak of MB would be appeared. However, the electrochemical signal of MB at ssDNA modified electrode greatly decreased after hybridizing with a complementary target DNA because the space structure of dsDNA blocks the interaction of MB with the guanine bases [26]. In fact, MB can be absorbed on the unbound guanine bases owing to the specific interaction between MB and the guanine bases. Thus, the electrochemical signals of MB on DNA modified electrode mainly depended on the amount of free bases (ssDNA) [26-28]. Fig. 5C presents the DPV voltammograms on the surface of MB-pDNA/Hb@AuNCs-G/AuNPs/GCE in Tris–HCl buffer (pH 7.0) solution containing 50 mM NaCl after being exposed to different concentrations of target cDNA (0, 0.1 fM, 1 fM, 10 fM, 100 fM, 1 pM, 10 pM). As seen, the DPV signal intensity of redox indicator drops during pDNA-cDNA hybridization because the MB molecules diffuse away from the modified electrode surface. Fig. 5D also shows a plot of current signal of MB, which decreases linearly with the target cDNA concentration in the range of 0.1 fM–10 pM. It is obvious that the signal for the reduction of MB after hybridization with cDNA decreased with the target concentration up to 0.1 pM. The linear regression equation of the calibration curve is expressed as $\Delta I\ (\mu A) = 0.5871 \log_{(cDNA)} (fM) + 0.8843$ with a correlation coefficient of 0.9944 (n = 8). The LOD of genosensor was found to be 0.037 fM.

The genosensor was assessed regarding its repeatability (intra-assay) and reproducibility (inter-assay). Good repeatability with a relative standard deviation (RSD) of 3.1% was found, upon the incubation of a 0.1 pM target DNA and submitting the same electrode to five successive DPV readings, with attention to removing the modified electrode from the electrochemical cell after each reading. For evaluation of the genosensor reproducibility, five individual modified electrodes were prepared under similar conditions and applied to the monitoring of 0.1 pM of target DNA. The outcomes showed a RSD of 7.4 % for DPV signals. The obtained results well confirmed that the repeatability and reproducibility of the genosensor are analytically acceptable.

### 3.5. Stability and selectivity of genosensor

In order to gain increased insight into the electrochemical performance of the genosensor, the stability of the modified electrode was investigated in this electrochemical bioassay. For this purpose, the MB-

pDNA/Hb@AuNCs-G/AuNPs/GCE was submerged in a Tris–HCl buffer solution (pH 7.0) for about 15 days and kept at 4 ˚C [25], after which the DPV peak current was found to decrease by only 3.1%, compared to its initial current, which shows an acceptable stability. When the modified electrode was kept at the room temperature (25 ˚C) for 15 days under the same conditions [25], only 8.7% of the DPV peak current was reduced. Such reasonable stability could be due to the nanoplatform stability and tight attachment of pDNA sequences to the surface of pDNA modified electrode.

The selectivity of the detection largely reflects the performance of the probe DNA. Thus, the genosensor specificity towards different DNA sequences was investigated using the DPV technique. As shown in Fig. 6, the significant reduction in MB signal intensity was observed in the presence of the target cDNA (0.1 pM), while the signal reduction was negligible in the presence of ncDNA (1.0 pM) and sbmDNA (1.0 pM) sequences. In fact, incubation of ncDNA and sbmDNA showed no significant change in the voltammograms of MB-pDNA/Hb@AuNC-G/AuNPs/GCE, suggesting that no hybridization is taking place. Thus, it was concluded that the immobilized DNA probe selectively binds to the target cDNA sequence. In addition, the effective discrimination against single-base mismatch was also observed. This observation indicates that the complete hybridization was not accomplished due to the base mismatch. The outcomes confirmed the selectivity and specificity of the genosensor towards the HPV16 DNA sequence.

### 3.6. PCR real sample bioassay

To investigate the practical applicability of the electrochemical genosensor for the actual real samples, we used the cDNA of clinical samples, with confirmed positive CML by PCR, as analyte [29]. The signal on-based genosensor was then applied to the quantitative determination of BCR/ABL fusion gene (target cDNA) of the positive CML patients according to the current biosensing strategy. The results were reported in Table 1. The results illustrated that this voltammetric genosensor possesses a high potential for the detection of BCR/ABL fusion gene in positive CML patients.

To further confirm the feasibility of genosensor, the “signal off” strategy assisted MB electrochemical signal probe was also applied to the quantitative determination of BCR/ABL fusion gene of the positive CML patients. The results reported in Table 2 presented that this impedimetric genosensor allows successful determination of target cDNA in CML patients.

## 4. Conclusions

The unique molecular characteristic of CML, the disease-causing ABL (9q34) to BCR (22q11) translocation, has provided an invaluable tool for disease diagnosis and monitoring of treatment response. Based on this fact, we designed a label-free electrochemical genosensor for the selective and sensitive determination of BCR/ABL fusion gene (target cDNA) of the positive CML patients. To design such sensor, the stable dispersions of graphene exfoliated in Hb@AuNCs solution were used for immobilization of pDNA on the AuNPs/GC electrode surface due to the high surface to volume ratio and functional groups of hemoglobin. Then, the target cDNA was detected on a Hb@AuNCs-G/AuNPs/GCE using the MB and $Fe(CN_6)^{3-/4-}$ electrochemical probes, for the “signal off” (DPV) and “signal on” (EIS) strategies, respectively. This genosensor showed acceptable analytical figures of merit in the terms of LOD, DLR, repeatability and reproducibility. In addition, the results presented that this electrochemical genosensor allows the successful determination of cDNA of clinical samples in CML patients. More importantly, our emphasis is placed on the novelty of nanoplatform design. Here, for the first time, the stable aqueous graphene dispersions synthesized through LPE of graphite powder in the presence of Hb@AuNCs. It is believed that Hb@AuNCs stabilized graphene through non-covalent bonding, which has certain advantages over stabilization through covalent bonding, such as minimal alterations in the structure and intrinsic properties of graphene [30]. Due to the increased advantages of this exfoliation method, LPE of graphene will become a significant technique in the not-so-distant future. This novel electrochemical nanoplatform can be used to detect other DNAs such as virus gene sequence.

## Declaration of competing interest

The authors declare the following financial interests/personal relationships which may be considered as potential competing interests: The authors gratefully acknowledge the support of this work by Iran National Science Foundation (INSF) (grant number: 98004333) and the Research Council of Razi University.

## Acknowledgements

The authors gratefully acknowledge the support of this work by Iran National Science Foundation (INSF) (grant number: 98004333) and the Research Council of Razi University.

## References

[1] A.P. Landstrom, A. Tefferi, Fluorescent in situ hybridization in the diagnosis, prognosis, and treatment monitoring of chronic myeloid leukemia, Leuk. Lymphoma 47 (2006) 397–402.
[2] S. Tashfeen, S. Ahmed, F.A. Bhatti, N. Ali, Real time polymerase chain reaction in diagnosis of chronic myeloid leukemia, J. Coll. Physicians Surg. Pak. 24 (2014) 190–193.
[3] F. Corrente, S. Bellesi, E. Metafuni, P.L. Puggioni, S. Marietti, A.M. Ciminello, T. Za, F. Sora, L. Fianchi, S. Sica, V. De Stefano, P. Chiusolo, Role of flow-cytometric immunophenotyping in prediction of BCR/ABL1 gene rearrangement in adult B-cell acute lymphoblastic leukemia, Cytomery B Clin. Cytom. 94 (2018) 468–476.
[4] K.Y.P.S. Avelino, R.R. Silva, A.G. da Silva Junior, M.D.L. Oliveira, C.A.S. Andrade, Smart applications of bionanosensors for BCR/ABL fusion gene detection in leukemia, J. King Saud Univ. 29 (2017) 413–423.
[5] J. Liu, X. Chen, Q. Wang, M. Xiao, D. Zhong, W. Sun, G. Zhang, Z. Zhang, Ultrasensitive monolayer $MoS_2$ field-effect transistor based DNA sensors for screening of Down syndrome, Nano Lett. 19 (2019) 1437–1444.
[6] M.B. Gholivand, A. Akbari, A sensitive electrochemical genosensor for highly specific detection of thalassemia gene, Biosens. Bioelectron. 129 (2019) 182–188.
[7] K.Y.P.S. Avelino, I.A. Morales Frias, N. Lucena-Silva, C.A.S. de Andrade, M.D.L. de Oliveira, Impedimetric gene assay for BCR/ABL transcripts in plasmids of patients with chronic myeloid leukemia, Microchim. Acta 185 (2018) 415.
[8] A. Soni, C.M. Pandey, S. Solanki, R.K. Kotnala, G. Sumana, Electrochemical genosensor based on template assisted synthesized polyaniline nanotubes for chronic myelogenous leukemia detection, Talanta 187 (2018) 379–389.
[9] K.Y.P.S. Avelino, I.A.M. Frias, N. Lucena-Silva, R.G. Gomes, C.P. de Melo, M.D.L. Oliveira, C.A.S. Andrade, Attomolar electrochemical detection of the BCR/ABL fusion gene based on an amplifying self-signal metal nanoparticle-conducting polymer hybrid composite, Colloids Surf. B Biointerfaces 148 (2016) 576–584.
[10] J.Y. Xia, J. Qing, J.J. Liu, A sensitive electrochemical impedance DNA biosensor based on ZnO nanorod electrodes for BCR/ABL fusion gene detection, Int. J. Electrochem. Sci. 14 (2019) 4271–4279.
[11] A. Soni, C.M. Pandey, S. Solanki, R.K. Kotnala, G. Sumana, Electrochemical genosensor based on template assisted synthesized polyaniline nanotubes for chronic myelogenous leukemia detection, Talanta 187 (2018) 379–389.
[12] K. Wang, C.L. Frewin, D. Esrafilzadeh, C. Yu, C. Wang, J.J. Pancrazio, M. Romero-Ortega, R. Jalili, C. Wallace, Neural recording: high-performance graphene-fiber-based neural recording microelectrodes, Adv. Mater. 31 (2019) 1970105.
[13] S. Ahadiana, M. Estilib, V.J. Suryac, J. Ramón-Azcóna, X. Lianga, H. Shikud, M. Ramalingama, T. Matsue, Y. Sakka, H. Bae, K. Nakajima, Y. Kawazoe, A. Khademhosseini, Facile and green production of aqueous graphene dispersions for biomedical applications, Nanoscale 7 (2015) 6436–6443.
[14] R.P. Shukla, R. Cazelles, D.L. Kelly, H. Ben-Yoav, A reduced-graphene oxide-modified microelectrode for a repeatable detection of antipsychotic clozapine using microliters-volumes of whole blood, Talanta 209 (2020) 120560.
[15] Q. He, S. Wu, S. Gao, X. Cao, Z. Yin, H. Li, P. Chen, H. Zhang, Transparent, flexible, all-reduced graphene oxide thin film transistors, ACS Nano 5 (2011) 5038–5044.
[16] N. Liu, F. Luo, H. Wu, Y. Liu, C. Zhang, J. Chen, One-step ionic-liquid-assisted electrochemical synthesis of ionic-liquid-functionalized graphene sheets directly from graphite, Adv. Funct. Mater. 18 (2008) 1518–1525.
[17] R. Narayan, J. Lim, T. Jeon, D.J. Li, S.O. Kim, Perylene tetracarboxylate surfactant assisted liquid phase exfoliation of graphite into graphene nanosheets with facile redispersibility in aqueous/organic polar solvents, Carbon 119 (2017) 555–568.
[18] Y. Hernandez, V. Nicolosi, M. Lotya, F.M. Blighe, Z. Sun, S. De, I.T. McGovern, B. Holland, M. Byrne, Y.K. Gun'Ko, J.J. Boland, P. Nairaj, G. Duesberg,

S. Krishnamurthy, R. Goodhue, J. Hutchison, V. Scardaci, A.C. Ferrari, J.N. Coleman, High-yield production of graphene by liquid-phase exfoliation of graphite, Nat. Nanotechnol. 3 (2008) 563–568.
[19] M. Shamsipur, L. Farzin, M.A. Tabrizi, F. Molaabasi, Highly sensitive label free electrochemical detection of VGEF165 tumor marker based on “signal off” and “signal on” strategies using an anti-VEGF165 aptamer immobilized BSA-gold nanoclusters/ionic liquid/glassy carbon electrode, Biosens. Bioelectron. 74 (2015) 369–375.
[20] C. Hu, D.P. Yang, Z. Wang, P. Huang, X. Wang, D. Chen, D. Cui, M. Yang, N. Jia, Biomimetically synthesized Ag@BSA microspheres as a novel electrochemical biosensing interface for sensitive detection of tumor cells, Biosens. Bioelectron. 41 (2013) 656–662.
[21] L. Farzin, M. Shamsipur, L. Samandari, S. Sadjadi, S. Sheibani, Biosensing strategies based on organic-scaffolded metal nanoclusters for ultrasensitive detection of tumor markers, Talanta 214 (2020) 120886.
[22] Y. Li, H.J. Schluesener, S. Xu, Gold nanoparticle-based biosensors, Gold Bull. 43 (2010) 29–41.
[23] K.R. Brown, A.P. Fox, M.J. Natan, Morphology-dependent electrochemistry of cytochrome c at Au colloid-modified SnO2 electrodes, J. Am. Chem. Soc. 118 (1996) 1154–1157.
[24] M. Sarparast, F. Molaabasi, R. Ghazfar, M.M. Ashtiania, M.B. Qaraid, A. Taherpoure, S.P. Amyab, M. Shamsipur, Efficient ethanol oxidation by hemoglobin-capped gold nanoclusters: the critical role of Fe in the heme group as an oxophilic metal active site, Electrochem. Commun. 103 (2019) 42–47.
[25] L. Farzin, S. Sadjadi, M. Shamsipur, S. Sheibani, Electrochemical genosensor based on carbon nanotube/amine-ionicliquid functionalized reduced graphene oxide nanoplatform fordetection of human papillomavirus (HPV16)-related head and neckcancer, J. Pharmaceut. Biomed. Anal. 179 (2020) 112989.
[26] J. Wang, F. Wang, S. Dong, Methylene blue as an indicator for sensitive electrochemical detection of adenosine based on aptamer switch, J. Electroanal. Chem. 626 (2009) 1–5.
[27] M. Shamsipur, L. Farzin, M.A. Tabrizi, M. Shanehsaz, CdTe amplification nanoplatforms capped with thioglycolic acid for electrochemical aptasensing of ultratraces of ATP, Mater. Sci. Eng. C 69 (2016) 1354–1360.
[28] C. Lin, Y. Wu, F. Luo, D. Chen, X. Chen, A label-free electrochemical DNA sensor using methylene blue as redox indicator based on an exonuclease III-aided target recycling strategy, Biosens. Bioelectron. 59 (2014) 365–369.
[29] M. Shamsipur, V. Nasirian, A. Barati, K. Mansouri, A. Vaisi-Raygani, S. Kashanian, Determination of cDNA encoding BCR/ABL fusion gene in patients with chronic myelogenous leukemia using a novel FRET-based quantum dots-DNA nanosensor, Anal. Chim. Acta 966 (2017) 62–70.
[30] T.S. Sreeprasad, V. Berry, How do the electrical properties of graphene change with its functionalization? Small 9 (2013) 341–350.